Enzymatic Characterization of the Full-Length and C-Terminally Truncated Hepatitis C Virus RNA Polymerases: Function of the Last 21 Amino Acids of the C Terminus in Template Binding and RNA Synthesis[†]

Nam Viet Vo, Jerry R. Tuler, and Michael M. C. Lai*

Department of Molecular Microbiology and Immunology, University of Southern California, Keck School of Medicine, Los Angeles, California 90033-1054

Received January 30, 2004; Revised Manuscript Received May 21, 2004

ABSTRACT: The nonstructural protein NS5B of hepatitis C virus (HCV) is an RNA-dependent RNA polymerase (RdRp), which plays a central role in viral replication. Most of the reported studies on HCV polymerase in vitro have used a truncated form of the enzyme lacking the C-terminal 21 amino acids (ΔC_{21}-NS5B). In this study, we compared the enzymatic properties of the full-length NS5B (FL-NS5B) and this truncated form. Removal of the C_{21} domain enhanced the enzyme stability. Both enzymes are capable of performing de novo and primer-dependent RNA syntheses, but each possesses a unique set of biochemical requirements for optimal RdRp activity. Whereas RNA synthesis by FL-NS5B remained relatively constant at 12−100 mM KCl, synthesis by ΔC_{21}-NS5B rapidly decreased at KCl concentrations greater than 12 mM. The different salt requirement for overall RNA synthesis by these two polymerases can in part be explained by the effect of monovalent ion concentration at the step of template binding, where binding by ΔC_{21}-NS5B but not FL-NS5B decreased proportionally as the KCl concentration increased from 25 to 200 mM. Thus, the C_{21} domain appears to contribute to NS5B−RNA template binding, probably through the hydrophobic stacking interaction between its aromatic amino acids and the nucleotide bases of the RNA. This interpretation was supported by the observation that the C_{21} polypeptide by itself could also bind to RNA to form binary complexes that were resistant to changes in the KCl concentration. Though both enzymes exhibited similar K_s values for each of the four NTPs (1−5 μM), ΔC_{21}-NS5B generally required lower NTP concentrations than FL-NS5B for optimal synthesis. Interestingly, ΔC_{21}-NS5B became severely inhibited at elevated NTP concentrations, which most likely is due to competitive binding of the noncomplementary nucleotide to the polymerase catalytic center. Finally, the terminal transferase activity of ΔC_{21}-NS5B was found to be distinct from that of FL-NS5B on several different RNA templates. Together, these findings indicated that the HCV NS5B C_{21} domain, in addition to being a membrane anchor, functions in template binding, NTP substrate selection, and modulation of terminal transferase activity.

The principal replicative enzyme of hepatitis C virus (HCV)[1] is a 66-kDa NS5B protein derived from the C terminal end of the viral polyprotein (*4*, *22*, *29*, *34*, *36*). NS5B was initially recognized as an RNA-dependent RNA polymerase (RdRp) by the presence of the hallmark GDD sequence, a motif involved in binding the Mg^{2+} ions essential for all polymerase functions (*22*). More direct evidence supporting NS5B RdRp enzymatic activity came from in vitro studies using purified recombinant NS5B expressed either in insect or bacterial cells (*4*, *29*, *34*). In vivo studies further confirmed the essential role of NS5B in HCV replication in cell cultures and in chimpanzees (*21*, *30*). NS5B has thus far been a major target for the development of antiviral therapy, an endeavor requiring detailed knowledge of the many complex biochemical properties of the enzyme.

X-ray crystallographic structure of NS5B reveals the canonical right-handed-like structure with domains representing fingers, the palm, and the thumb as seen in other polymerases (*6*, *27*). NS5B possesses an unusual feature in that its finger and thumb domains interact extensively, resulting in the O structure rather than the U structure typically observed for other polymerases. The only other known polymerase with this O-shaped architecture is the ϕ6 viral RdRp (*7*). The other novel structural feature of NS5B is a β-hairpin motif protruding from the thumb domain toward the active site that locates at the base of the palm domain. This structure, together with some part of the NS5B C terminus, has been shown to modulate NS5B initiation site selection in RNA synthesis (*16*, *39*). Chemical cross-linking and yeast two-hybrid analyses further suggest that NS5B exists and functions in a higher oligomeric form (*47*).

HCV NS5B by itself can initiate RNA chain synthesis through two distinct mechanisms. On most RNA templates

[†] This work was partially supported by an NIH Grant AI 47348.

* To whom correspondence should be addressed: 2011 Zonal Avenue, HMR-401, Los Angeles, California 90033-1054. Phone: 323-442-1748. Fax: 323-442-1721. E-mail: michlai@hsc.usc.edu.

[1] Abbreviations: RdRp, RNA-dependent RNA polymerase; DdRp, DNA-dependent RNA polymerase; HCV, hepatitis C virus; BVDV, bovine viral diarrhea virus; TNTase, terminal transferase.

10.1021/bi049773g CCC: $27.50
Published on Web 07/20/2004

examined, NS5B requires an existing primer for initiating RNA synthesis. Such priming either comes from exogenously added primer or intramolecularly from the 3′ end of RNA, which base pairs with another region on the same molecule (*4*, *11*, *29*). On certain RNA templates, NS5B can carry out de novo RNA synthesis (*11*, *20*, *35*), where it catalyzes two free NTPs to form a dinucleotide product and subsequently extends it into longer RNA chains. NS5B also synthesizes RNA in a nontemplated manner, in which it incorporates nucleoside monophosphates onto the 3′ end of the RNA, a reaction akin to that performed by terminal nucleotidyl transferases (*38*). The ability of the HCV polymerase to synthesize RNA using various RNAs as templates shows a lack of binding selectivity and suggests that other viral and or host protein factors are required for selective replication of the HCV genome. Indeed, HCV NS5B alone exhibits little template-binding specificity, except for some RNA aptamers isolated from the SELEX procedure (*5*, *45*).

NS5B, expressed either alone or in the context of the entire HCV polyprotein, has been demonstrated to be a membrane-bound protein, mostly associating with the endoplasmic reticulum (ER) (*17*, *41*) or lipid raft (*42*). Hydropathy profiles of the NS5B amino acid sequence reveal the last 21 C-terminal amino acids to be highly hydrophobic, and truncation studies demonstrate that these amino acids are responsible for transmembrane anchorage of NS5B (*18*, *41*). Fusion of the C-terminal 21 amino acids of NS5B to a heterologous green fluorescent protein is necessary and sufficient to target it to the ER membrane (*41*). For these reasons, most in vitro characterization of the HCV polymerase was done using purified NS5B missing the C-terminal 21 amino acid (C_{21}) domain to increase its solubility and thus ease of purification. Though ΔC_{21}-NS5B still possesses in vitro RdRp activity, removal of the C_{21} hydrophobic domain either by deletion or a premature stop codon is deleterious for viral replication in vivo (*26*). More importantly, replacement of this hydrophobic domain by a related transmembrane sequence derived from bovine viral diarrhea virus (BVDV) did not rescue HCV replication (*26*). These findings suggest essential functions of the NS5B C_{21} domain other than being a membrane anchor. Here, we characterized both the FL-NS5B and ΔC_{21}-NS5B to further understand the enzymatic properties of the HCV polymerase and elucidate additional functional roles of the C terminus. Our studies revealed that deletion of the C_{21} domain affected template binding, NTP substrate selectivity, and terminal transferase (TNTase) activity of the HCV polymerase; thus, the C_{21} domain is likely functionally involved in the enzymatic processes of HCV replication.

EXPERIMENTAL PROCEDURES

Materials. Reagents were purchased from the following sources: [α-^{32}P]NTP and [γ-^{32}P]GTP (NEN); HPLC-grade nucleoside triphosphates and glycogen (Pharmacia, now Amersham Biosciences); T7 Shortscript In Vitro Transcription Kit (Ambion); betaine (Sigma); oligonucleotides (USC/Norris Microchemical Core Facility); homopolymeric RNA poly(rA), poly(rC), poly(U) (Pharmacia, now Amersham Biosciences); poly(rG) (Sigma); C_{21} peptide, WFPLCLLLLS-VGVGIYLLPNR (WM Keck Foundation Biotechnology Resource Laboratory at Yale University).

Purification of HCV NS5B. The recombinant NS5B derived from the NS5B NIH1b strain was purified from the *DH5*α *Escherichia coli* strain by the method of Vo et al. (*45*). The full-length and the C_{21}-truncated NS5B contained 591 and 570 native amino acids, respectively, and a tag of six histidines at the N terminus of the protein for the purpose of affinity chromatographic purification.

Preparation of RNA Templates. Large quantities of RNA templates were made from runoff transcription reactions using the T7 promoter containing PCR DNA templates and reagents from the Ambion's T7 Shortscript In Vitro Transcription Kit. These RNA templates were purified from a 9.5% denaturing polyacrylamide gel (PAG). RNA concentration was determined spectrophotometrically. The PCR DNA templates containing the T7 promoter were prepared using the oligonucleotide T7-TMOAR/D (3′-CCTCACCCCAC-CCACCACCCCGGGCCCAAACAACAACAA ACAAGTC-GACCACCACTCGCGGGATATCACTCAGCATAAT-5′) and a combination of an upstream primer (5′-GGAGTG-GGGTGGGTGGTGGG-3′) and a downstream primer (3′-GTCGACCACCACTCGCGGGATATCACTCAGCATAAT-CTTAAGG-5′). The core T7 promoter sequence is underlined. Transcription from this PCR DNA using the T7 RNA polymerase yielded a 62-nucleotide runoff RNA product, TMOA, which was used as a template for NS5B RdRp assay. To make a complementary RNA, we synthesized a PCR product that contained the T7 promoter at the opposite end of the transcribed sequence; we also used this T7-PCR DNA template to produce [γ-^{32}P]GGA RNA primer using [γ-^{32}P]GTP and ATP. The primer was purified by excision from a 23% denaturing PAGE.

NS5B RdRp Assay. In a standard 20-μL reaction, 2 μM NS5B was incubated with 2.5 μM RNA template and 100 μM NTP in NS5B transcription buffer (50 mM HEPES at pH 7.3, 10 mM $MgCl_2$, 10 mM β-mercaptoethanol, 50 mM KCl, 100 mM betaine, 0.05% Tween-20, and 10 μg/mL acetylated bovine serum albumin). Deviations from this standard assay condition were noted in the figures and figure captions when the effects of salt, $MgCl_2$, pH, and Tween-20 were tested by titrations of each of these components. For de novo RNA synthesis, [γ-^{32}P]GTP (1 mM, $\sim 10^3$ cpm/pmole) was used to terminally label the RNA product. For primer-dependent RNA synthesis, [γ-^{32}P]GGA primer (10 μM, 1000−2000 cpm/pmol) was used. The reactions were incubated at 30 °C for a desired period of time and stopped by phenol extraction, and the RNA products were precipitated using ethanol in the presence of 0.5 mg/mL glycogen as a carrier. The precipitated pellet was dried down and dissolved in formamide loading buffer (FLB; 89 mM Tris-borate at pH 8.3, 2.5 mM EDTA, 0.05% xylene cyanol and bromophenol blue dyes, 10 mM EDTA, and 80% freshly deionized formamide). The dissolved RNA samples were heated at 100 °C for 3 min and resolved on a 23% (38:2 acrylamide/bisacrylamide) PAG containing 8 M urea. Gel electrophoresis was performed using the TBE buffer (89 mM Tris-borate at pH 8.3 and 2.5 mM EDTA). After electrophoresis, the gels were directly exposed to a phosphorimager screen and scanned using a Molecular Dynamic PhosphorImager. To obtain a conversion factor between phosphorimager counts and femtomoles of RNA, known amounts of the labeling nucleotide solution of a given specific activity were spotted on the same gel and exposed to the phosphorimager screen.

K_s Determination. The apparent K_s values for each of the four NTP were determined for FL-NS5B and ΔC_{21}-NS5B enzyme by assays using four variants of the TMOA RNA templates as described previously (*46*). The NS5B enzyme concentration used in these experiments (2 μM) is in the linear range of the reaction rate (data not shown). The K_s value for UTP determined using homopolymeric template was done by incubating a 20-μL reaction containing 6 pmol of NS5B enzyme, 54 pmol of oligo U_{12}, and 10 pmol of poly(rA) (465−660 nucleotides) in NS5B transcription buffer and various concentrations of [α-^{32}P]UTP (0.1−20 μM, ~7000 cpm/pmol) at 30 °C for 40 min. Similar reactions were done to determine the K_s value for GTP, except [α-^{32}P]GTP (0.5−30 μM, ~17000 cpm/pmole), 10 pmol of oligoG_{12} and 1 pmol of poly(rC) (246−646 nucleotides) were used. The RNA product of the reaction was precipitated by addition of 80 μL of a YEP (0.5 mg/mL yeast tRNA carrier, 50 mM EDTA, and 50 mM NaPPi) solution and 400 μL of 100% TCA (trichloroacetic acid), followed by incubation on ice for 15 min. The TCA-precipitated product was collected on a Whatman glass membrane (GF/C), washed with 5 mL of an ice-cold 1 M HCl and 0.1 M NaPPi solution, rinsed with ethanol, dried, and counted in the scintillation counter.

Assay for TNTase Activity. A total of 2 μM NS5B was preincubated with 2.5 μM TMOA RNA template in a 20-μL reaction. The reaction was initiated by adding a single [α-^{32}P]NTP (0.1 mM, 5000 cpm/pmole) and incubated at 30 °C for 60 min. The 5′-end ^{32}P-labeled RNA markers were made from runoff transcription using the PCR templates containing the T7 promoter, T7 RNA polymerase, and [γ-^{32}P]GTP. The RNA products were analyzed on 23% denaturing PAG and quantified as described above.

RNA Binding and Dissociation Assays. In a standard 20-μL reaction, 1 pmol of NS5B was incubated with 0.5 pmol of ^{32}P-labeled gel-purified RNA (10 000−32 000 cpm/pmol) in NS5B transcription buffer in various KCl concentrations. A total of 2 pmol of ^{32}P-labeled RNA and 4 nmol of C_{21} peptide were used in the KCl titration experiment. The reaction was incubated at 30 °C for 3 min, filtered via a nitrocellulose membrane under vacuum, washed with 1 mL of NS5B transcription buffer, dried, and counted. For dissociation kinetic studies, the NS5B protein and the ^{32}P-labeled RNA were first incubated together at 30 °C for 2 min to reach binding equilibrium (data not shown). The reaction volume was then diluted 10-fold in the presence of 60-fold excess, by mass, of unlabeled competitor poly(U) RNA. This condition mimicked an irreversible first-order dissociation kinetic reaction because any dissociated NS5B was prevented from reassociating with the ^{32}P-labeled RNA by the excess poly(U). Indeed, in a control reaction in which the poly(U) was mixed with the ^{32}P-labeled RNA prior to the addition of the NS5B enzyme, only background binding of ^{32}P-labeled RNA was noted (data not shown). Aliquots of the reaction were filtered through a nitrocellulose membrane at various time points to trap the bound complexes on the membrane and filter through the unbound labeled RNA. The membrane was washed with 1 mL of NS5B transcription buffer, dried, and counted. For saturation binding experiments, NS5B in the amount of 25, 50, 100, 200, 500, 1000, and 2000 fmol were titrated against a constant 50 fmol of ^{32}P-labeled RNA in a 20-μL reaction. The reaction mixture was incubated at 30 °C for 2 min, filtered via a nitrocellulose membrane under vacuum, washed with 1 mL of NS5B transcription buffer, dried, and counted. The apparent binding constant, K_d, was determined as the concentration of enzyme that gave half the level of saturated binding.

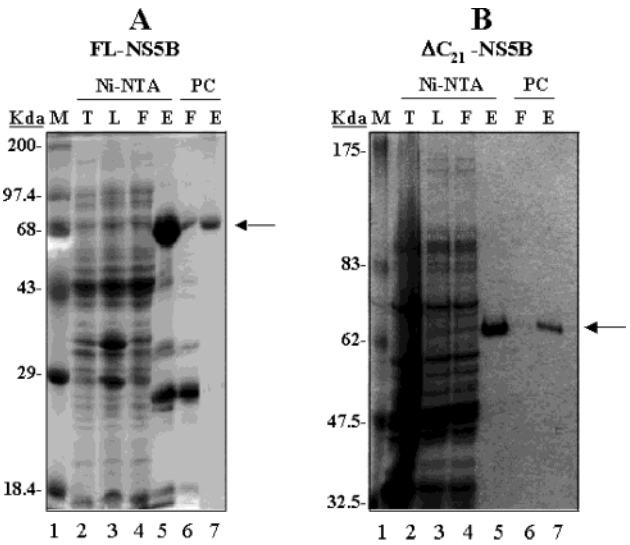

FIGURE 1: SDS−PAGE protein profile of HCV polymerase purification. FL-NS5B (A) and ΔC_{21}-NS5B (B) were purified using the same procedure as described in the Experimental Procedures, first by affinity Ni−NTA chromatography (lanes 3−5), followed by phosphocellulose ion-exchange chromatography (lanes 6 and 7). The protein fractions were resolved on 8% PAG and visualized by Coomassie blue staining. Lane 1, protein marker; lane 2, whole-cell mixture; lane 3, Ni−NTA cell lysate loading fraction; lane 4, Ni−NTA flow-through fraction; lane 5, Ni−NTA-eluted fraction; lane 6, phosphocellulose flow-through fraction; lane 7, phosphocellulose-eluted fraction.

RESULTS

Rationale. Basic biochemical knowledge of the steps involved in the complex process of RNA synthesis by the HCV polymerase is essential to the development of its effective theurapeutic inhibitors. Here, we performed comparative studies of two forms of the HCV polymerase, a full-length and a truncated NS5B missing the last 21 C-terminal amino acids. Our aim is to further understand the enzymatic properties of the HCV polymerase, especially to uncover additional functions of the C_{21} terminal domain. The reason for the latter lies in the observation that deletion of NS5B C_{21} terminus is deleterious to HCV replication in vivo (*26*), yet most of the in vitro polymerase assays involving HCV NS5B were performed using ΔC_{21}-NS5B. Although ΔC_{21}-NS5B exhibits in vitro RdRp activity, so far it has been unclear whether there exist any enzymatic differences between this truncated enzyme and the FL-NS5B. To compare their in vitro RdRp enzymatic activities, we expressed the bacterial recombinant proteins, FL-NS5B and ΔC_{21}-NS5B and purified them by Ni−NTA affinity chromatography (lanes 3−5 of Figure 1), followed by ion-exchange phosphocellulose chromatography (lanes 6 and 7 of Figure 1). Both proteins were subjected to identical expression and purification procedures, giving rise to the final purity of more than 90% as judged by Coomassie blue-stained SDS−PAGE (Figure 1).

Comparison of RdRp Activity of FL-NS5B and ΔC_{21}-NS5B. We first examined the RdRp activities of the two NS5B

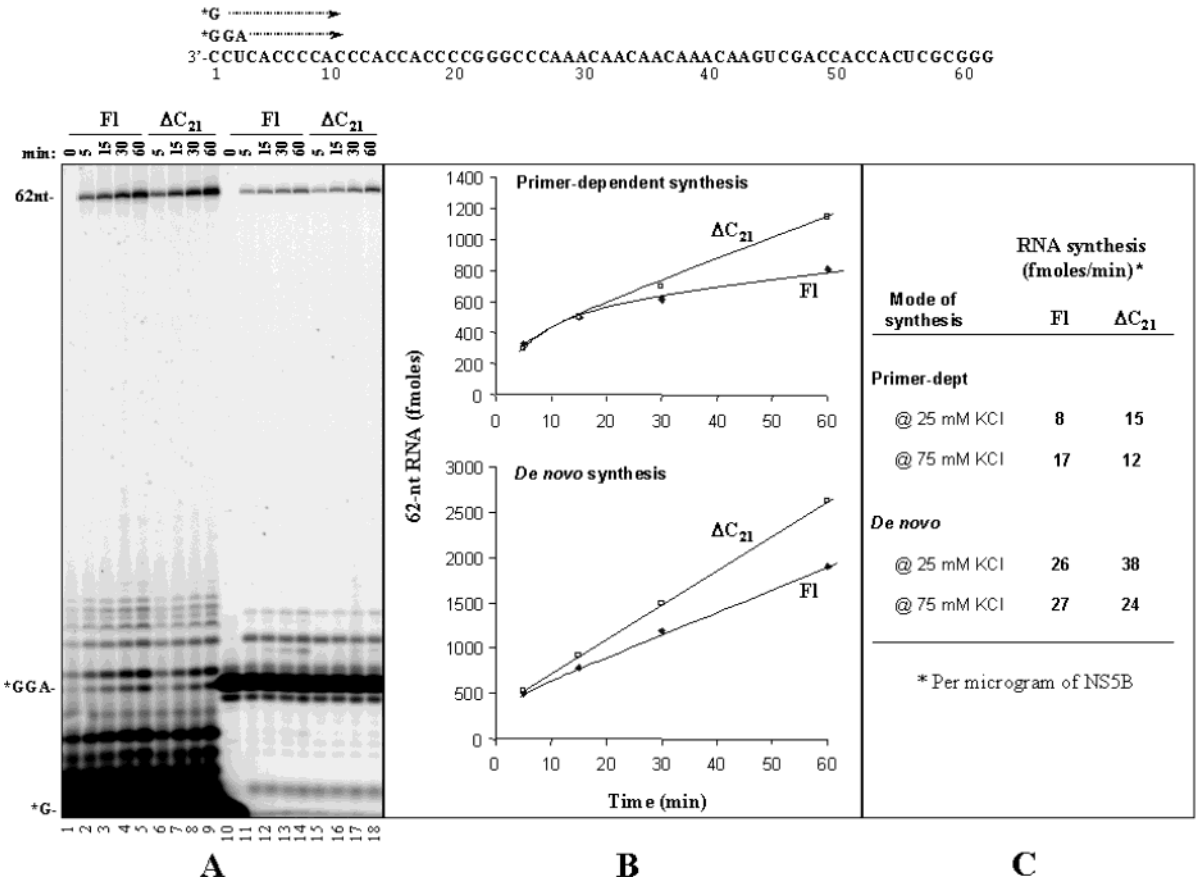

FIGURE 2: Kinetics of RNA synthesis by HCV full-length and truncated polymerase. (A) Gel analysis of RNA products from de novo (lanes 1−9) or primer-dependent synthesis (lanes 10−18) by FL-NS5B (lanes 2−5 and 11−14) and ΔC_{21}-NS5B (lanes 6−9 and 15−18). RNA products from 0-, 5-, 15-, 30-, and 60-min time points are shown. (B) Kinetic profiles of the synthesis of 62-nucleotide full-length RNA product from primer-dependent (top) or de novo synthesis (bottom) by the full-length (□) and truncated (◆) NS5B. (C) Relative enzyme-specific activities of full-length and truncated NS5B at different KCl concentrations and modes of initiation.

enzymes to determine if they exhibit any differences in their ability to synthesize RNA. We employed an in vitro RdRp assay in which a 62-nucleotide synthetic TMOA RNA (top of Figure 2) served as a template for the HCV polymerase to generate a full-length complementary RNA product either through de novo RNA synthesis with [γ-^{32}P]GTP (lanes 1−9 of Figure 2A) or primer-dependent synthesis using [γ-^{32}P]-GGA as a primer (lanes 10−18 of Figure 2A). As previously demonstrated (*46*), this simple well-defined HCV RdRp assay system allows us to examine two different initiation modes of RNA synthesis. Both enzymes are capable of de novo (lanes 1−9 of Figure 2A), and primer-dependent synthesis (lanes 10−18 of Figure 2A), generating a single runoff 62-nucleotide full-length RNA product and a number of shorter RNA products in the 2−6-nucleotide range. The nature of these short products, be they abortive products or products initiated from sites other than the 3′ RNA terminus, remained to be investigated. It is notable that both enzymes generated identical patterns of RNA products, with no detectable intermediate RNA products between the short 2−6 nucleotides and the 62 nucleotide full length, suggesting that both the full-length and the truncated forms are processive polymerases, at least for the RNA templates 62 nucleotides long. Our recent results using a longer template (320 nucleotides) and heparin as a trapping agent suggest that HCV polymerase is also processive on this longer template (data not shown). In these reactions, where 1 mM [γ-^{32}P]GTP was used for de novo synthesis and 0.01 mM [γ-^{32}P]GGA was used for primer-dependent synthesis, higher rates of de novo than primer-dependent synthesis were observed for both enzymes (Figure 2C). However, the relative rates of primer-dependent versus de novo synthesis closely depend on the GTP and GGA primer concentrations used (Figure 5B and data not shown).

At 25 mM KCl, both NS5B forms displayed a similar initial rate of full-length RNA synthesis, either via de novo (first 5 min of the bottom graph of Figure 2B) or primer-dependent synthesis (first 15 min of the top graph of Figure 2B). As synthesis reached a steady-state level later in the reaction, the rate of synthesis by FL-NS5B was lower than that by ΔC_{21}-NS5B (Figure 2B). These trends, however, reversed when a higher KCl concentration (75 mM) was used (Figure 2C and Figure 3C), indicating that recycling of FL-NS5B for synthesis is poor at low salt (25 mM KCl), a likely result of enzyme aggregation in the presence of the hydrophobic C_{21} domain in a low ionic environment. This idea was supported by an additional observation that addition of detergent (0.05% Tween 20) to the reaction enhanced RNA synthesis by FL-NS5B much more (8-fold) than ΔC_{21}-NS5B (3-fold) (Table 1 and data not shown). Stimulation of RNA synthesis by the presence of 0.05% Tween-20 could be due to the lessening of FL-NS5B protein aggregation at low KCl or the prevention of the hydrophobic protein from sticking to the sides of the reaction tube.

Biochemical Requirements for Optimal RdRp Activity of FL-NS5B and ΔC_{21}-NS5B. We further examined the effects

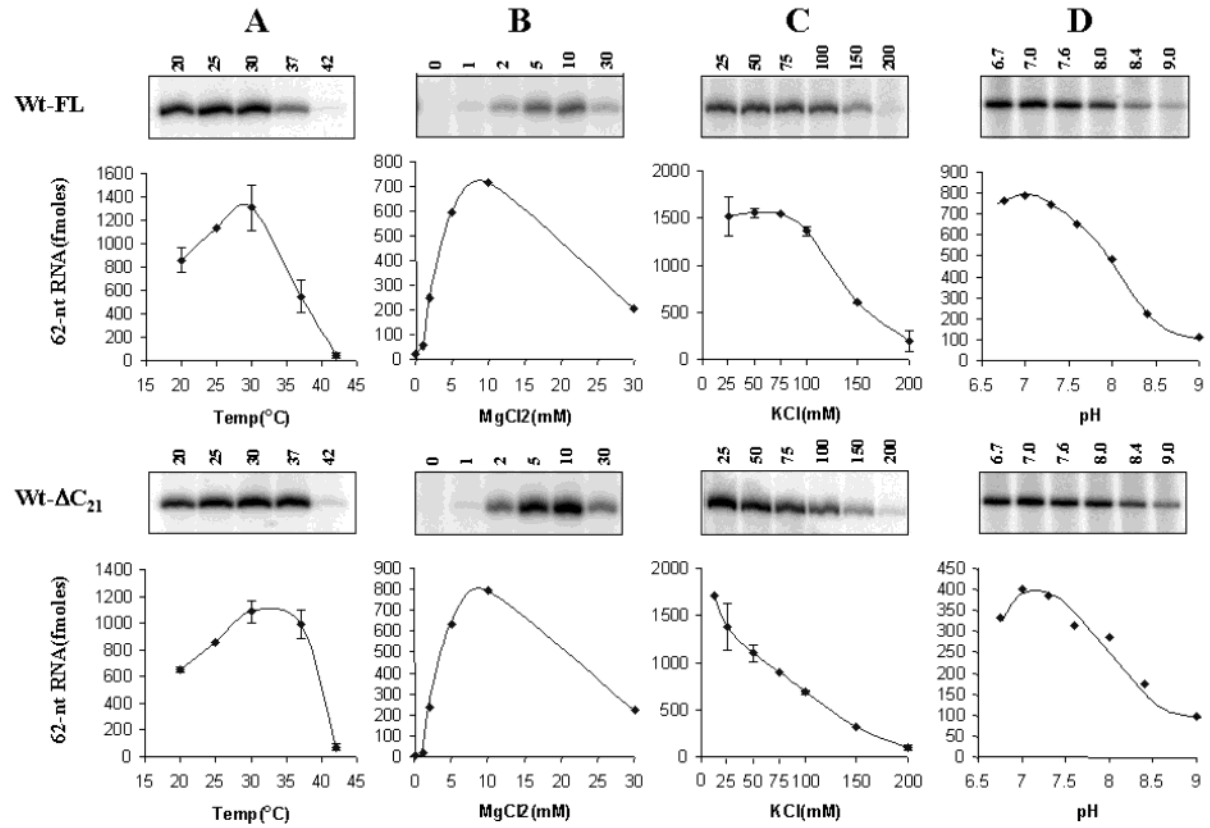

FIGURE 3: Biochemical requirement for optimal RNA synthesis by full-length NS5B (top) and truncated NS5B (bottom). Effect of temperature (A), $MgCl_2$ concentration (B), KCl concentration (C), and pH (D) on the synthesis of the 62-nucleotide full-length RNA product from the TMOA template. The reactions were done as described in the Experimental Procedures.

Table 1: Optimal Reaction Condition for RNA Synthesis

reaction condition	FL-NS5B	ΔC_{21}-NS5B
temperature	30 °C	30−37 °C
pH	7	7
KCl	25−75 mM	≤12.5 mM
$MgCl_2$	10 mM	10 mM
Tween-20 (0.05%)	8×	3×

of some basic reaction components essential for the enzymatic activities of most RNA polymerases, including temperature, monovalent cations, divalent cations, pH, and NTP substrate concentration. We investigated the effect of each of these components on the de novo RNA synthesis by NS5B using the TMOA template. Both FL- and ΔC_{21}- NS5B RdRp activities increased ~1.5-fold as the temperature of the reaction increased from 20 to 30 °C (Figure 3A). As the reaction temperature increased to 37 °C, synthesis by the full-length enzyme sharply dropped, while synthesis by the ΔC_{21} enzyme remained roughly at the level obtained at 30 °C. The RdRp activity of both forms was almost completely lost at 42 °C. Incubation of the free enzyme on ice also inactivated the FL-NS5B much more readily than the ΔC_{21}-NS5B enzyme (data not shown). Thus, removal of the C_{21} domain enhances the stability of the enzyme.

The effect of monovalent cations on the overall RNA synthesis by FL-NS5B and ΔC_{21}-NS5B is shown in Figure 3C. Synthesis by FL-NS5B remained constant within the 25−100 mM KCl range, above which synthesis steadily declined until it almost completely disappeared at 200 mM KCl. In contrast, maximum synthesis by ΔC_{21}-NS5B occurred at 12 mM KCl or less and, as KCl increased above 12 mM, synthesis proportionally decreased. Similar results were obtained when NaCl was used (data not shown). As described shortly below, the reduction of RNA synthesis by ΔC_{21}-NS5B at high salt largely reflects the effect of poor template binding by this enzyme in an elevated ionic environment.

While removal of the C_{21} domain affected the monovalent ion requirement of NS5B, it did not appear to alter the divalent metal cation requirement. RNA synthesis showed a sharp maximum of activity at 10 mM $MgCl_2$ for both forms of NS5B (Figure 3B). Synthesis increased rapidly as the $MgCl_2$ concentration increased from 1 to 10 mM, above which the effect became inhibitory. Both enzymes showed an absolute requirement for the divalent metal ion because the absence of Mg^{2+} resulted in no detectable RNA synthesis.

The effect of pH on RNA synthesis by both NS5B enzymes is shown in Figure 3D. RNA synthesis by both enzymes shows a fairly sharp pH optimum, which centered at pH 7. Above pH 7.5, RNA synthesis by both enzymes dropped rapidly, particularly more so by FL-NS5B. For example, RNA synthesis by the ΔC_{21} enzyme at pH 8 is 38% and pH 9 is 25% of that at pH 7, while synthesis by the FL enzyme at pH 8 is 25% and pH 9 is 13% of that at pH 7. The dependence of RNA synthesis on pH in this pH range is probably due to an ionization of one or more amino acid residue(s) in the NS5B protein, which alters template and/or substrate binding, and not an ionization of the substrate because magnesium-nucleoside triphosphate complexes have no p*K* in this range. A comparison of the optimal reaction condition for each of these two NS5B enzymes is summarized in Table 1.

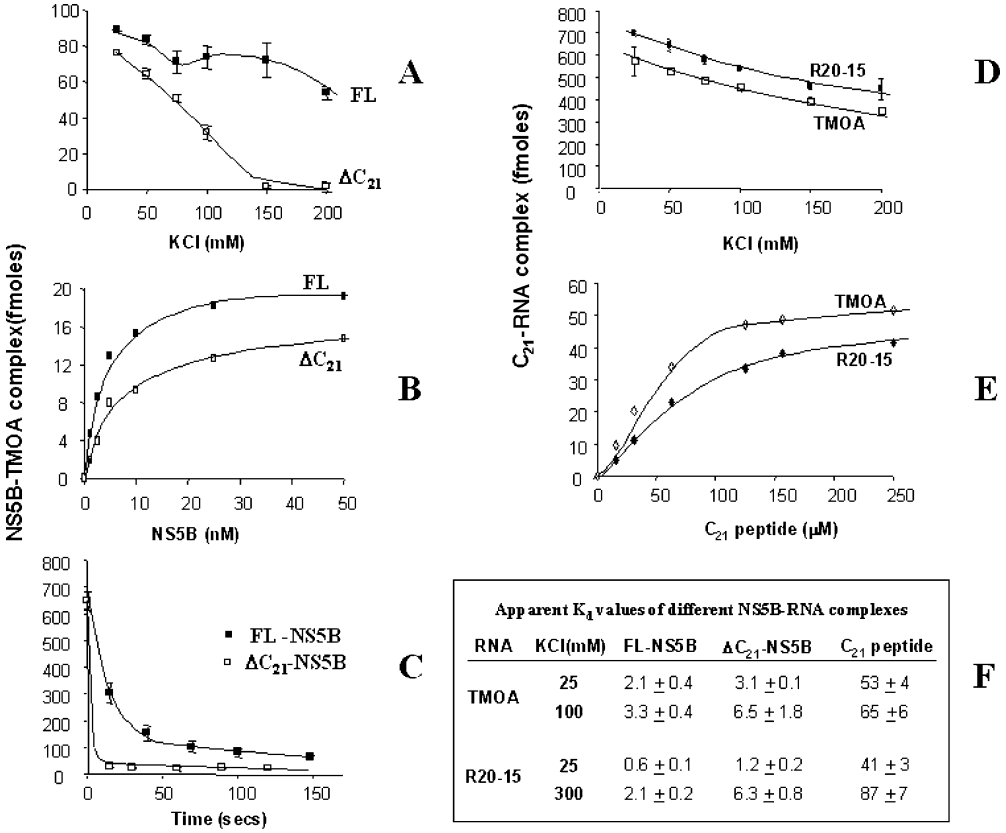

Apparent K_d values of different NS5B-RNA complexes — F

RNA	KCl(mM)	FL-NS5B	ΔC_{21}-NS5B	C_{21} peptide
TMOA	25	2.1 ± 0.4	3.1 ± 0.1	53 ± 4
	100	3.3 ± 0.4	6.5 ± 1.8	65 ± 6
R20-15	25	0.6 ± 0.1	1.2 ± 0.2	41 ± 3
	300	2.1 ± 0.2	6.3 ± 0.8	87 ± 7

FIGURE 4: Template binding by HCV NS5B and the C_{21} synthetic peptide. All binding experiments shown here used filter binding assays described in the Experimental Procedures. (A) Effect of KCl concentration on template binding by HCV full-length and truncated polymerase. Binding between TMOA RNA template and HCV polymerase at various KCl concentrations was allowed to reach binding equilibrium at 30 °C for 3 min, and the complexes were collected on a nitrocellulose membrane. (B) Saturation binding experiment using the TMOA template and varied concentrations of HCV NS5B. The binding constant K_d for each enzyme was extrapolated from the binding curve as the NS5B concentration that gave half-maximal binding. (C) Dissociation kinetics of complexes of NS5B and TMOA RNA. Preformed NS5B−TMOA complexes were diluted 10-fold in volume with the excess competitor poly(U) to determine the rate of dissociation. The *x* axis is the time in seconds after dilution, and the *y* axis is femtomoles of the existing NS5B−TMOA complex. (D) Effect of KCl concentration on template binding by the synthetic C_{21} peptide and TMOA RNA (□) or R20-15 RNA (■). (E) Saturation binding experiment to determine K_d value for binding between C_{21} peptide and TMOA RNA (□) or R20-15 RNA (■). (F) Apparent K_d values of binding of NS5B and C_{21} peptide to different RNA templates in different KCl concentrations. K_d values in nanomolars are shown for truncated and full-length NS5B and in micromolars for the C_{21} peptide.

RNA Template Binding by FL-NS5B and ΔC_{21}-NS5B. Reduction of the overall RNA synthesis by the truncated NS5B in the presence of a higher KCl concentration may be due to the salt effect at one or a combination of steps during the RNA synthesis cycle. In this study, we focused on examing the effect of salt concentration on the step of template binding by using two RNA templates, TMOA and R20-15. TMOA is a 62-nucleotide minimally structured RNA, consisting of a single loop and a 6-bp stem joined by a 3′ single-stranded sequence. R20-15 is an 87-nucleotide highly structured SELEX RNA aptamer that binds NS5B strongly and selectively (*45*). We employed the filter-binding assay to follow the formation of the binary complex between NS5B and ^{32}P-labeled RNA at various KCl concentrations. Association of both NS5B enzymes to either TMOA or R20-15 RNA occurred extremely rapidly, reaching binding equilibrium as soon as they are mixed together even at 0 °C (data not shown). At low KCl concentrations (≤25 mM), FL-NS5B displays slightly higher RNA-binding affinity than ΔC_{21}-NS5B (parts A and F of Figure 4). However, as KCl concentrations increased up to 150 mM, binding of ΔC_{21}-NS5B to TMOA RNA decreased proportionally until no complex formation was observed at KCl concentrations above 150 mM. In contrast, titration of 25−200 mM KCl only slightly affected the binding of FL-NS5B to TMOA RNA (Figure 4A). Similar results were obtained for R20-15 RNA binding by the two NS5B enzymes, except that higher KCl concentrations (200−300 mM) were needed to see the effect (data not shown). Binding constants determined from the saturation binding experiments (parts B and F of Figure 4) also showed that the truncated enzyme binds RNA with lower affinity than its full-length counterpart at elevated KCl concentrations.

These data suggest that ΔC_{21}-NS5B binds RNA mostly via polar interactions, while FL-NS5B binds RNA through both polar and nonpolar interactions. This interpretation was further confirmed by the KCl effect on dissociation kinetics of the NS5B−RNA binary complex, where the NS5B−RNA complexes were first formed at 25 mM KCl, and then their kinetics of dissociation were followed by diluting the reaction volume 10-fold in the presence of 75 mM KCl and poly(U) competitor. Initially, dissociation was rapid in which the majority of the complexes was disrupted within the first minute, suggesting that this group of complexes is fairly unstable and held mostly by ionic interactions between the enzyme and RNA (Figure 4C). Over the next several minutes, however, a much lower rate of dissociation occurred, indicating that this group of complexes is more stable. The

Table 2: K_s Value Comparison of FL-NS5B and ΔC_{21}-NS5B

Template/primer	Nucleotide	K_s (μM) FL	K_s (μM) ΔC_{21}
5'-GGA 3'-CCUUA...	ATP	5.0 ± 0.8	5.7 ± 1.9
5'-GGA 3'-CCUCA...	GTP	4.9 ± 1.3	5.4 ± 1.4
5'-GGA 3'-CCUGA...	CTP	3.5 ± 1.7	2.9 ± 1.2
5'-GGA 3'-CCUAU...	UTP	0.6 ± 0.1	0.7 ± 0.2
oligo rG poly (rC)	GTP	2.0 ± 0.1	2.2 ± 0.1
oligo U poly (rA)	UTP	24 ± 6	26 ± 7

latter complexes are probably stabilized by nonionic forces because they were not sensitive to changes in the ionic environment. As shown in Figure 4C, elevated KCl concentrations disrupted the binary complexes of ΔC_{21}-NS5B and RNA much more readily than those of FL-NS5B. Thus, the C_{21} hydrophobic domain appears to assist NS5B in RNA binding through certain nonpolar interactions.

Many single-stranded nucleic acid binding proteins bind their target templates via hydrophobic stacking interactions between their aromatic amino acids and the bases of the nucleotides of the template (*9*, *15*, *32*). Intriguingly, the NS5B C_{21} domain, (**R**A**R**P**RWF**MLCLLLLSVGVGI**Y**LLPN**R**, shown here as the underlined sequence), also contains three aromatic amino acids flanked by the basic amino acid arginines, presumably for neutralization of the negatively charged phosphate groups of D/RNA. This prompted us to test whether the synthetic C_{21} polypeptide can bind RNA. Indeed, the C_{21} polypeptide by itself could interact with either the TMOA or R20-15 RNA template, though binding affinity of this polypeptide was much lower than that of the FL-NS5B or ΔC_{21}-NS5B (parts E and F of Figure 4). In the control reaction in which similar concentrations of BSA were tested for binding to these RNAs, only background signals were detected (data not shown). As predicted, formation of the complex between RNA and C_{21} polypeptide was not affected significantly by changes in KCl concentrations (Figure 4D), further supporting the idea that it interacts with RNA through nonpolar contacts.

NTP Requirement: C Terminus Is Required To Suppress the Effect of Substrate Inhibition at High NTP Concentrations. To test whether the absence of the C_{21} domain affects the affinity of NTP binding, we determined the apparent K_s of each of the four NTPs for the two NS5B enzymes. The initial steady-state rates were determined at various concentrations for each of the four NTPs as described (*46*), and the K_s value for each nucleotide was determined (Table 2). Both NS5B enzymes displayed similar K_s for each of the four NTPs, with the K_s values ranging from 1 to 5 μM when heteropolymeric RNA sequences were used in the RdRp assay. These K_s values fall within the range of K_s values reported for NS5B previously (*8*). Thus, the absence of the C_{21} domain does not affect the affinity of NS5B for its NTP substrate. Intriguingly, K_s values for UTP determined from heteropolymeric RNA and that from poly(rA)/oligoU were profoundly different, 0.6−0.7 μM for the heteropolymeric RNA and 24−26 μM for the homopolyadenylate. Such a disparity reflects the different NTP affinities of NS5B at different RNA template sequences.

To further investigate how the NTP concentration influences the overall de novo RNA synthesis from the TMOA template by the two NS5B enzymes, we performed titration of each of the four NTPs up to millimolar concentration range, while keeping the other three nucleotides at a constant concentration of 0.1 mM. RNA synthesis by FL-NS5B showed broad UTP and CTP optima, ranging from 100 to 1000 μM (top graphs of panels C and D of Figure 5). In contrast, ΔC_{21}-NS5B showed much sharper UTP and CTP optima, where synthesis peaked at a much lower concentration range of 10−100 μM. Both enzymes required much greater GTP and ATP concentrations than CTP or UTP for optimal RNA synthesis, with synthesis by FL-NS5B peaking at 3000 μM ATP and 5000 μM GTP and synthesis by ΔC_{21} enzyme reaching a maximum at 500 μM ATP and 3000 μM GTP (parts A and B of Figure 5). Experiments in which a combination of ATP, CTP, and UTP were titrated also revealed that RNA synthesis by the truncated enzyme decreased at NTP concentrations above 0.5 mM, while synthesis by the full-length enzyme remained relatively unaffected at concentrations of NTP up to 3 mM (data not shown). Thus, optimal synthesis by ΔC_{21}-NS5B requires markedly lower NTP concentrations than that by FL-NS5B (Table 3).

GTP and ATP are required for the formation of the first four nucleotides of the RNA product from de novo synthesis using the TMOA template starting at its 3′ terminus (see the top of Figure 2); this fact most likely explains the higher GTP and ATP concentrations than the UTP or CTP concentration requirement. Interestingly, UTP is required as the fifth nucleotide substrate, yet neither of the two NS5B forms needed high UTP concentrations for efficient synthesis, indicating that a high concentration of the first 3−4 NTP substrate is important for initiation of de novo RNA synthesis by the HCV polymerase. This interpretation was further supported by the observation that only low concentrations of GTP and ATP (10−100 μM) were needed for optimal synthesis when [γ-^{32}P]GGA primer was used to bypass de novo initiation (top of Figure 2 and data not shown). Consistent with findings from earlier reports (*8*, *31*), these results suggest that HCV polymerase requires a much higher NTP substrate concentration for initiating de novo RNA synthesis than elongating RNA chain.

Above the optimal NTP concentration, RNA syntheses by both FL- and ΔC_{21}-NS5B became inhibited. This phenomenon is known as NTP substrate inhibition, which has been thought to occur when the excess incorrect nucleotide enters the active site of the polymerase and interferes with the binding of the correct complementary nucleotide substrate (*10*, *40*). Figure 5 clearly shows that the ΔC_{21} enzyme encountered substrate inhibition at a much lower NTP concentration than the full-length enzyme. For example, while synthesis by FL-NS5B remained relatively unaffected by CTP or UTP concentrations up to 3000 μM, synthesis by the truncated enzyme became inhibited at CTP or UTP concentrations above 100 μM and mostly diminished at 3000 μM. Similarly, synthesis by FL-NS5B increased with ATP

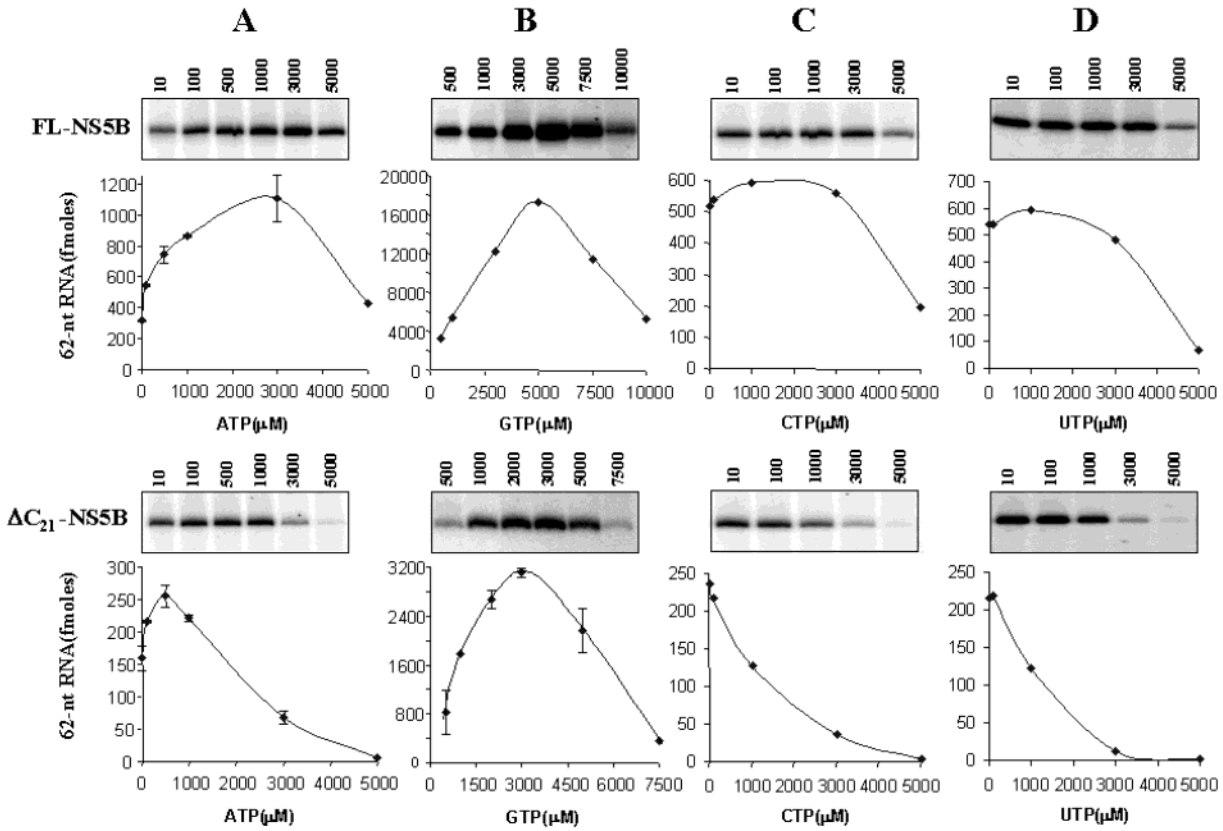

FIGURE 5: NTP requirement for optimal RNA synthesis by full-length (top) and truncated (bottom) NS5B. Effect of varying ATP (A), GTP (B), CTP (C), and UTP (D) on the synthesis of the 62-nucleotide full-length RNA product from the TMOA template. These titration experiments were done as described in the Experimental Procedures, where the concentration of one nucleotide triphosphate was changed, while the concentrations of the other three nucleotides were kept at a constant 0.1 mM.

Table 3: Optimal NTP Concentration for RNA Synthesis

	optimal concentration (μM)	
NTP	FL-NS5B	ΔC_{21}-NS5B
ATP	3000	500
GTP	5000	3000
CTP	1000	10
UTP	1000	100

concentrations up to 3000 μM, and only beyond this concentration did inhibition occur; the truncated enzyme, on the other hand, became inhibited at ATP concentrations only above 500 μM. It is interesting that, although both enzymes showed identical K_s values for NTP, they did not share the same NTP concentration requirement for optimal synthesis. However, K_s values only reflect general affinity, not selectivity.

Earlier studies of *E. coli* DdRp have shown that excess noncomplementary nucleoside triphosphates inhibited synthesis of polynucleotides when templates of restricted base composition were employed (*10*, *40*). We adopted this strategy to further confirm the substrate inhibition effect using the poly(rC)/oligo(rG) as the template/primer for the HCV polymerase. In this assay, incorporation of labeled GMP was measured in the absence or presence of the unlabeled noncomplementary substrate competitor ATP or CTP. As shown in Figure 6, the rate of GMP incorporation by both forms of NS5B reached a maximum at GTP concentrations above 5−10 μM in the absence of the noncomplementary NTP competitor. In the presence of high concentrations (5 mM) of ATP or CTP, GMP incorporation became significantly inhibited, particularly more so with the truncated NS5B (Figure 6B) than its full-length counterpart (Figure 6A). This inhibition was significantly relieved as GTP concentrations increased in the reaction catalyzed by FL-NS5B (Figure 6A). In contrast, ATP or CTP inhibition of GMP incorporation by ΔC_{21}-NS5B was only marginally relieved by higher GTP concentrations, further confirming that the removal of the C_{21} domain of NS5B affects NTP selectivity and leads to substrate inhibition at high NTP concentrations.

C_{21} Domain Also Influences TNTase Activity of NS5B. In addition to templated RNA synthesis, HCV NS5B can add NMP to the 3′ end of an RNA template in a nontemplated manner. Ranjith-Kumar and co-workers have demonstrated that this TNTase-like activity is an inherent function of the HCV polymerase, which requires the same GDD motif involved in normal templated synthesis. Because the NS5B C_{21} domain appears to be involved in the normal templated RNA synthesis, we tested whether it is also involved in the NS5B TNTase activity. For this, reactions were done by incubating single α-^{32}P-labeled NTP (rATP, rGTP, rCTP, or rUTP) with purified, NTP-free RNA templates and NS5B. While both polymerases can add up to 30−40 nucleosides on the 3′ terminus of RNA (Figure 7 and Figure 8), the ΔC_{21}-NS5B enzyme displayed altered TNTase activities on several different RNAs. Adenylyl transferase activity of the full-length enzyme was much higher than that by the truncated NS5B when TMOA RNA was used (lane 2 versus lane 6 of Figure 7A). In contrast, GMP addition by the truncated enzyme was slightly higher than that by the full-length NS5B

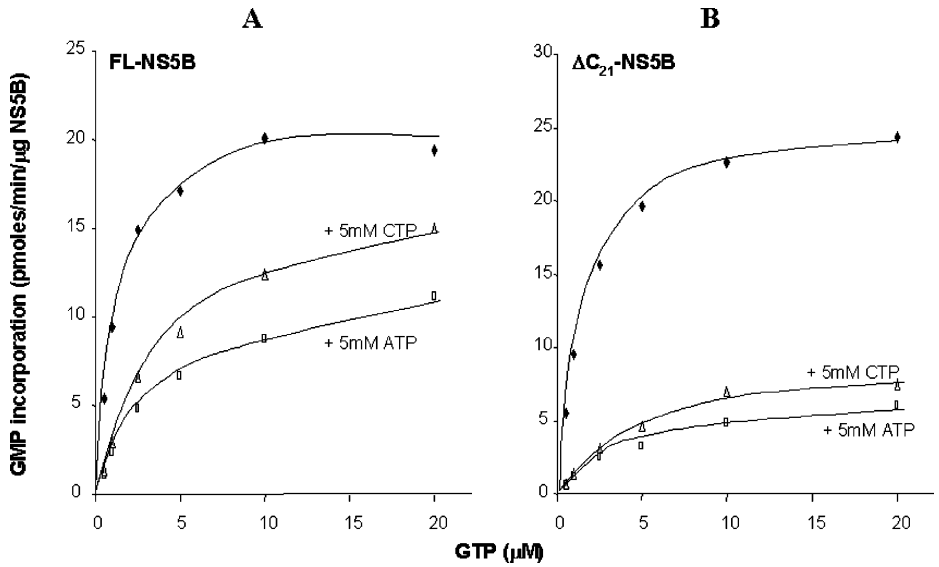

FIGURE 6: Inhibitory effect of noncomplementary nucleotides on RNA synthesis by the full-length (A) and truncated (B) NS5B using the homopolymeric (C) template. [α-^{32}P]GMP incorporation was measured at various GTP concentrations in the absence of a noncomplementary NTP (◆), in the presence of 5 mM noncomplementary unlabeled ATP (□), or 5 mM noncomplementary unlabeled CTP (△). The *x* axis is the micromolar concentration of GTP, and the *y* axis is the GMP incorporation in picomoles of GTP per minute per microgram of NS5B.

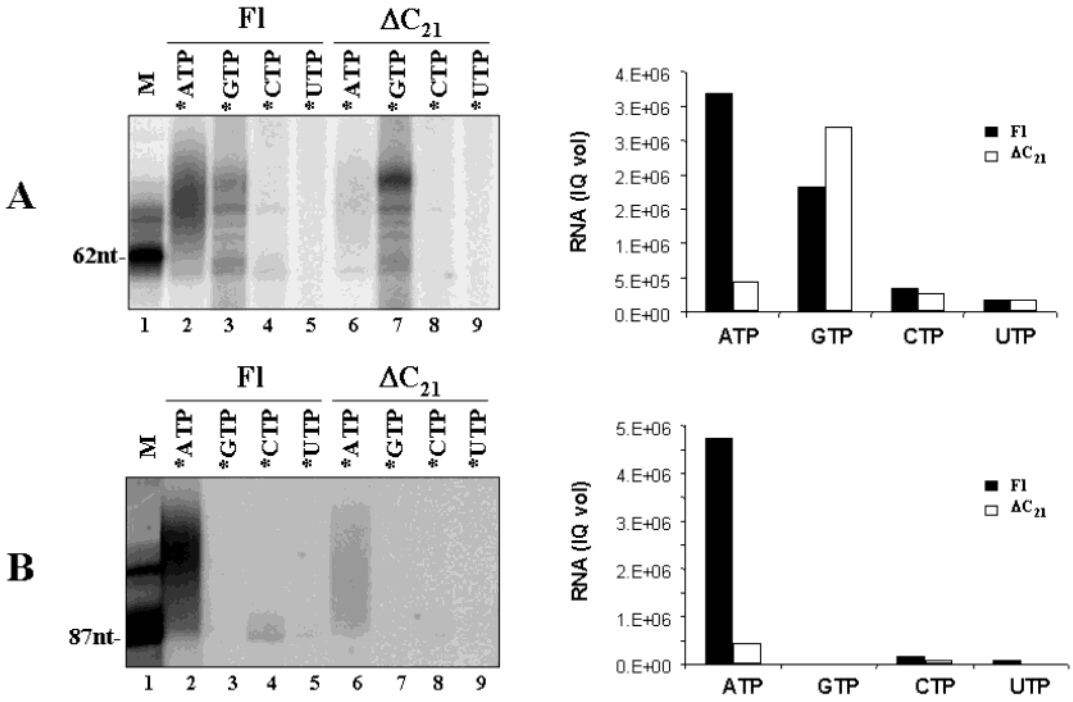

FIGURE 7: Terminal nucleotidyl transferase activity of the full-length versus truncated NS5B. Nucleotide addition at the 3′ terminus of 62-nucleotide TMOA RNA (A) or 87-nucleotide R20-15 RNA (B) by FL-NS5B (lanes 2−5) and ΔC_{21}-NS5B (lanes 6−9). NS5B was incubated with the RNA template in the presence of 0.1 mM of each of the four α-^{32}P-labeled NTP. The RNA marker is shown in lane 1. Quantitation of the amount of incorporation of each NMP is shown next to each gel profile. The *y* axis is the amount of NMP addition in arbitrary ImageQuant units.

(lane 3 versus lane 7 of Figure 7A). Both enzymes also added CMP and UMP at the 3′ end of TMOA, but these reactions occurred at a reduced level as compared to their purine nucleotide counterparts.

Both NS5B proteins also catalyzed AMP incorporation at the 3′ end of two other RNA templates, R20-15 (lanes 2 and 6 of Figure 7B) and GGA template (Figure 8B), but AMP addition by the truncated enzyme consistently occurred at a much lower extent than that by the full-length NS5B. Titration of high ATP concentrations did not rescue the low AMP TNTase activity of ΔC_{21}-NS5B on two different RNA templates (Figure 8). The TNTase activity of NS5B did not add the 4 NMP equally, and the efficiency of each NTP depended on the template sequence. For example, neither NS5B form displayed GMP TNTase activity at the 3′ end of R20-15 RNA (lanes 3 and 7 of Figure 7B), but both enzymes showed robust guanylyl transferase activity on the TMOA template. This is consistent with the findings reported earlier, which showed that TNTase specificity depends on the sequence at the 3′ end of the RNA (*38*). Overall, the full-length enzyme exhibited greater TNTase activities than the truncated NS5B, suggesting that the C_{21} domain also has

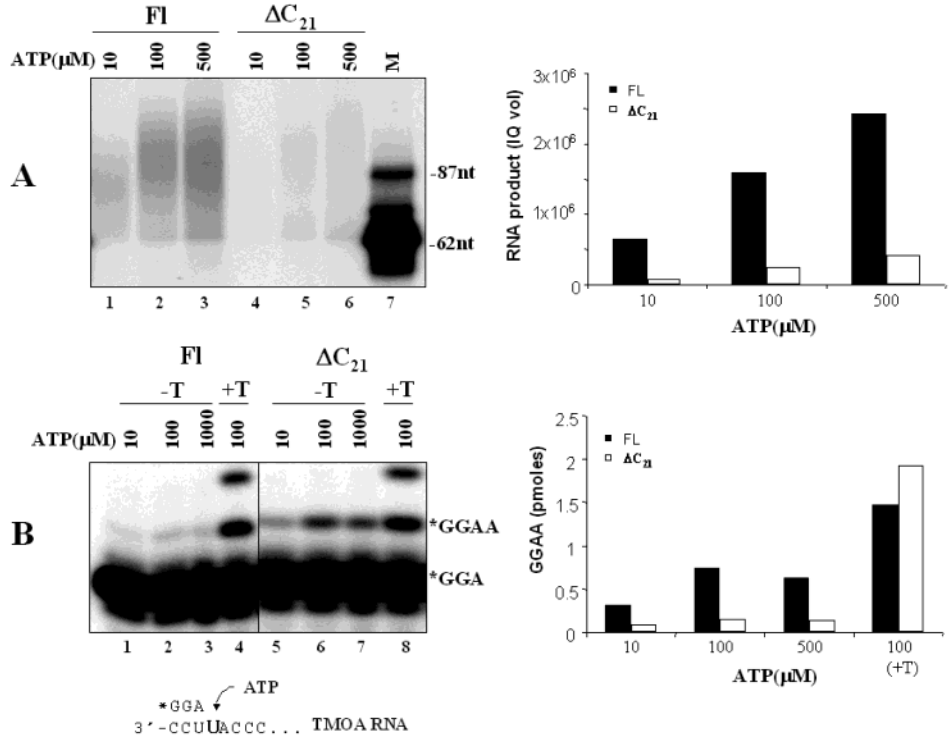

FIGURE 8: Effect of increasing the ATP concentration on AMP addition at the 3′ terminus of 62-nucleotide TMOA RNA (A) or 3-nucleotide GGA RNA primer (B) by FL-NS5B and ΔC_{21}-NS5B. NS5B was incubated with the RNA template in the presence of increasing [α-^{32}P]-ATP concentrations as stated. Quantitation of AMP incorporation is shown on the right. (A) Lane 7 is the RNA size marker. (B) lanes 4 and 8 are templated-dependent AMP incorporation at 0.1 mM ATP in the presence of the TMOA template, in which the GGA RNA oligo annealed at the TMOA 3′ terminus and served as a primer (see bottom of B). Lanes 1−3 and 5−7 are AMP incorporation by NS5B at the 3′ end of GGA primer in the absence of the TMOA template. −T denotes reactions with the primer only, and +T denotes reactions with both the template and primer.

some functional role in the TNTase activity of the HCV polymerase.

DISCUSSION

Most of the in vitro polymerase assays for HCV so far have used an HCV polymerase lacking the C-terminal 21 amino acids. It is not clear whether this truncated form reflects the authentic enzymatic activity of the native full-length NS5B. Furthermore, it has been shown that truncation of more than 21 amino acids (39−60 amino acids) of the HCV NS5B C-terminal region vastly improved its RdRp activity (3−15-fold) (*1*, *12*, *28*). These findings suggest that the C-terminal sequences are not essential for the enzymatic activity but may have regulatory functions. However, most of these studies were done without consideration of the possible differences in biochemical requirements for optimal RdRp activity among different polymerase forms. In addition, the percentage of active enzyme molecules in each polymerase preparation might be different for different forms of polymerase. Thus, it was difficult to evaluate from the published studies the functional significance of the C-terminal regions. In this study, we used the purified FL-NS5B and ΔC_{21}-NS5B enzyme fractions that contain a similar percentage of active molecules (~1%) (data not shown) using an RdRp assay in which RNA synthesis was limited to a single round by addition of heparin as a competitor after initiation had occurred. We showed that FL-NS5B and ΔC_{21}-NS5B are both capable of either de novo or primer-dependent RNA synthesis at similar efficiency, but their optimal RdRp activities varied significantly with different biochemical conditions. The ΔC_{21}-NS5B polymerase generally needed lower concentrations of monovalent ion and NTP substrates than FL-NS5B for maximal synthesis, though both enzymes shared similar divalent metal ion (10 mM $MgCl_2$) and pH optima (pH 7). We found that ΔC_{21}-NS5B displayed reduced template binding at high concentrations of monovalent ions, had lower RNA synthesis at elevated NTP concentrations, and possessed altered TNTase activity. In addition, we found that the presence of the C_{21} peptide affected the stability of the enzyme. Reconstitution experiments in which the NS5B C_{21} polypeptide was mixed with the ΔC_{21}-NS5B enzyme either before or after addition of an RNA template did not reverse these effects (data not shown).

Our studies revealed the potential existence of two distinct classes of NS5B−RNA binary complexes. One class appeared to be stabilized mostly by ionic interactions and readily dissociated upon treatment with higher KCl concentrations. The other class of complexes is resistant to changes in KCl concentration and thus must be held together largely by nonionic forces. Interestingly, our findings also suggest that the hydrophobic C_{21} domain contributes substantially to both the ionic and nonionic interactions between NS5B and RNA. First, the binary complexes of ΔC_{21}-NS5B−RNA dissociate much more rapidly than the FL-NS5B−RNA complexes as the ionic strength of the reaction increased. Second, the C_{21} domain by itself can bind RNA to form complexes that are resistant to concentration changes of KCl. Aromatic ring stacking interactions between the nucleotide bases and aromatic amino acid side chains have been demonstrated to be important for single-stranded nucleic acid

and protein interactions (*9*, *32*). These aromatic residues are often clustered or flanked by basic amino acids, which presumably serve in charge neutralization (*15*). Intriguingly, there exists in the C_{21} domain three aromatic amino acids, tryptophan, phenylalanine, and tyrosine, flanked by the basic arginine residues. Our results suggest that these amino acids also interact with the bases of the RNA template in a manner similar to other single-stranded nucleic acid interacting proteins. Template-binding properties of full-length polymerase variants carrying mutations at these aromatic amino acids will be investigated in our future studies.

The role of the C_{21} domain, which spans amino acids 570−591 of NS5B, in template binding is also interesting in light of recent reports (*1*, *28*) on the amino acid residues between 545 and 570, which occupy the putative RNA-binding cleft of the HCV NS5B. Together with our studies, these results suggest that the C-terminal amino acid sequence from 545 to 591 constitutes part of the NS5B−RNA-binding site. A number of protein factors involved in gene expression also possess nucleic acid binding domains within their C termini. These include the microbial transcription factor NusG, whose X-ray crystal structure revealed the C terminus with a KOW sequence motif embedded in a structurally conserved RNA-binding element (*44*). The C terminus of the mammalian heterogeneous nuclear ribonucleoprotein A1 also contains a number of aromatic amino acids and binds single-stranded RNA (*23*). Recent analysis of the tomato bushy stunt virus replicase also showed that one of its RNA-binding domains resides in the C terminus, and this region also contains aromatic amino acids flanked by basic residues (*14*, *37*). Thus, the HCV polymerase probably belongs to a broad class of enzymes that interact with single-stranded nucleic acid through a C-terminal tail.

RNA synthesis by HCV polymerase is inhibited at elevated concentrations of NTP. Such inhibition could be due to chelation of Mg^{2+} metal ions at elevated NTP concentrations (1−5 mM). This possibility can be ruled out because a much higher concentration of $MgCl_2$ (10 mM) was present in our reaction. A more likely explanation of this substrate inhibition effect comes from the model of NTP geometric selection and induced fit proposed for other polymerases (*24*, *40*). According to this model, nucleotide selectivity of the polymerase generally proceeds by weak binding of all possible substrates at a common active site on the enzyme, followed by a conformational change to form a much stronger complex only when the correct NTP aligns itself opposite the complementary template base, and finally formation of the phosphodiester bond. Kinetic and structural studies revealed that DNA polymerases bind correct dNTPs with about 10−1000-fold higher affinity than they bind incorrect dNTPs and that formation of the phosphodiester bond occurs at a much faster rate for correct nucleotides than incorrect ones (*24*). Substrate inhibition occurs when a high concentration of incorrect nucleotides effectively competes with the correct complementary nucleotide for binding to the enzyme active center (*40*). When this happens, the polymerase either misincorporates the incorrect nucleotide, probably at a much slower rate, or removes the incorrect nucleotide to make room for the correct substrate. Either way, the overall synthesis slows down or becomes inhibited if the NTP concentration becomes too high.

We found that elevated NTP concentrations (>3 mM) severely inhibited RNA synthesis by ΔC_{21}-NS5B synthesis but only marginally inhibited the synthesis by FL-NS5B. Thus, the C_{21} domain of NS5B also seems to be involved in NTP selection, possibly through one or a combination of steps proposed in the induced-fit model discussed above. The C_{21} domain may constitute part of the structural geometry of the NS5B active site necessary for optimal NTP selectivity, or it may function in assisting the removal of incorrect NTP once they are bound to the active center. Alternatively, the C_{21} domain may regulate the catalysis of phosphodiester bond formation, such that in the absence of the C_{21} domain, the enzyme would misincorporate incorrect NMP into the RNA product. Further kinetic and structural analyses are needed to resolve these possibilities. In sum, this model best explains the inhibitory effect at high NTP concentrations associated with the deletion of the C_{21} domain and the probable functional role of the C_{21} domain in NTP selection. A recent report by Ranjith-Kumar and co-workers proposed that the amino acids 43−51 from the C-terminal tail of NS5B interacts with the β loop to regulate GTP selection and de novo RNA synthesis (*39*). The physical proximity of the C_{21} sequence to these C-terminal amino acids may further support the idea that the C_{21} domain itself constitutes part of the active site of the HCV polymerase.

Besides its probable function in template binding and NTP selectivity, the C_{21} domain also modulates the TNTase of HCV polymerase. This is evident from the observation that, while both the FL-NS5B and ΔC_{21}-NS5B possess TNTase activity, the truncated polymerase generally exhibits lower TNTase activities on several RNA templates, particularly the addition of AMP. Recent studies clearly show that the TNTase activity is an inherent property of the BVDV and HCV polymerases and requires the same RdRp GDD motif (*38*). Other viral polymerases, including BMV, turnip crinkle virus, and poliovirus replicases, have also been reported to add nucleotides to the 3′ terminus of either the template or product RNA (*3*, *13*, *43*). In fact, a number of DdRps have been reported to add nontemplated nucleotides to the 3′ end of the RNA (*2*, *19*, *33*). Thus, the ubiquitous association of the TNTase activity with many viral RdRps may suggest certain inherent biological functions. It is possible that TNTase-mediated addition of extra nucleotides at the 3′ end of the viral genome helps protect it from damage by cellular exonucleases. Alternatively, TNTase activity may serve to repair a 3′ terminal deletion of genomic or antigenomic viral RNA. Finally, when extra nucleotides are added at the 3′ end, TNTase activity may regulate de novo RNA-chain initiation because, for HCV polymerase, the 3′-end initiation is preferred over internal initiation (*16*, *48*).

It has long been thought that the sole function of the hydrophobic C_{21} domain of the HCV polymerase is to anchor this enzyme to the membrane. Though NS5B is a membrane-associated protein by itself, it has never been directly demonstrated to submerge in the membrane layer in the replication complex in vivo. It is conceivable that other proteins are involved to anchor the replication machinery to the membranous site in which NS5B situates away from the membrane. Our studies presented here are consistent with the finding that replacement of the HCV NS5B C_{21} hydrophobic domain by a related transmembrane sequence derived from BVDV failed to support HCV replication, suggesting

the sequence-specific requirement of this domain (*26*). Altogether, the experimental data suggest that this domain constitutes part of the enzyme active center, where it is involved in interacting with the RNA template, selecting the correct NTP substrate, and modulating RNA synthesis. On the other hand, if NS5B is anchored to the membrane via its C_{21} domain in the replication complex, then RNA synthesis by NS5B would occur at least partially submerged in the membrane compartment. Thus, the C_{21} domain can both interact with the membrane and serve as a structural constituent of the polymerase active center. Alternatively, the C_{21} segment is not a constituent of the polymerase active-site architecture; rather, the observed effects associated with the deletion of the C_{21} domain were due the disturbance of the structural integrity of NS5B. Further investigation, e.g., X-ray crystal structural determination of the full-length enzyme, will be necessary to distinguish between these two possibilities. Regardless of which mechanism is involved, our findings provided some explanation as to why deletion of NS5B C_{21} is deleterious for HCV replication in vivo. The absence of this domain would not only interfere with the membrane localization of the enzyme, but also affect its interaction with the RNA template in a relatively high intracellular salt concentration of the mammalian cell (~150 mM) (*25*). In the presence of a high millimolar range of physiological NTP concentrations, removal of the NS5B C_{21} domain would also lead to inhibition of RNA synthesis as well as TNTase activity, which may be essential for HCV replication.

ACKNOWLEDGMENT

We thank Dr. Caroline Kane and Salvatore Cilia of University of California, Berkeley, for critically reading the paper.

REFERENCES

1. Adachi, T. H., Ago, N., Habuka, K., Okuda, M., Komatsu, S., Ikeda, and Yatsunami, K. (2002) The essential role of C-terminal residues in regulating the activity of hepatitis C virus RNA-dependent RNA polymerase, *Biochim. Biophys. Acta 1601*, 38−48.
2. Altmann, C. R., Solow-Cordero, D. E., and Chamberlin, M. J. (1994) RNA cleavage and chain elongation by *Escherichia coli* DNA-dependent RNA polymerase in a binary enzyme. RNA complex, *Proc. Natl. Acad. Sci. U.S.A. 91*, 3784−3788.
3. Arnold, J. J., Ghosh, S. K., and Cameron, C. E. (1999) Poliovirus RNA-dependent RNA polymerase (3D(pol)). Divalent cation modulation of primer, template, and nucleotide selection, *J. Biol. Chem. 274*, 37060−37069.
4. Behrens, S. E., Tomei, L., and De Francesco, R. (1996) Identification and properties of the RNA-dependent RNA polymerase of hepatitis C virus, *EMBO J. 15*, 12−22.
5. Biroccio, A., Hamm, J., Incitti, I., De Francesco, R., and Tomei, L. (2002) Selection of RNA aptamers that are specific and high-affinity ligands of the hepatitis C virus RNA-dependent RNA polymerase, *J. Virol. 76*, 3688−3696.
6. Bressanelli, S., Tomei, L., Roussel, A., Incitti, I., Vitale, R. L., Mathieu, M., De Francesco, R., and Rey, F. A. (1999) Crystal structure of the RNA-dependent RNA polymerase of hepatitis C virus, *Proc. Natl. Acad. Sci. U.S.A. 96*, 13034−13039.
7. Butcher, S. J., Grimes, J. M., Makeyev, E. V., Bamford, D. H., and Stuart, D. I. (2001) A mechanism for initiating RNA-dependent RNA polymerization, *Nature 410*, 235−240.
8. Carroll, S. S., Sardana, V., Yang, Z., Jacobs, A. R., Mizenko, C., Hall, D., Hill, L., Zugay-Murphy, J., and Kuo, L. C. (2000) Only a small fraction of purified hepatitis C RNA-dependent RNA polymerase is catalytically competent: Implications for viral replication and in vitro assays, *Biochemistry 39*, 8243−8249.
9. Casas-Finet, J. R., Khamis, M. I., Maki, A. H., and Chase, J. W. (1987) Tryptophan 54 and phenylalanine 60 are involved synergistically in the binding of *E. coli* SSB protein to single-stranded polynucleotides, FEBS *Lett. 220*, 347−352.
10. Chamberlin, M. J. A. B., P. (1964) Mechanism of RNA polymerase action: Characterization of the DNA-dependent synthesis of polyadenylic acid, *J. Mol. Biol. 8*, 708−726.
11. Crotty, S., Maag, D., Arnold, J. J., Zhong, W., Lau, J. Y., Hong, Z., Andino, R., and Cameron, C. E. (2000) The broad-spectrum antiviral ribonucleoside ribavirin is an RNA virus mutagen, *Nat. Med. 6*, 1375−1379.
12. Ferrari, E., Wright-Minogue, J., Fang, J. W., Baroudy, B. M., Lau, J. Y., and Hong, Z. (1999) Characterization of soluble hepatitis C virus RNA-dependent RNA polymerase expressed in *Escherichia coli*, *J. Virol. 73*, 1649−1654.
13. Guan, H., and Simon, A. E. (2000) Polymerization of nontemplate bases before transcription initiation at the 3′ ends of templates by an RNA-dependent RNA polymerase: An activity involved in 3′ end repair of viral RNAs, *Proc. Natl. Acad. Sci. U.S.A. 97*, 12451−12456.
14. Hearne, P. Q., Knorr, D. A., Hillman, B. I., and Morris, T. J. (1990) The complete genome structure and synthesis of infectious RNA from clones of tomato bushy stunt virus, *Virology 177*, 141−151.
15. Helmann, J. D., and Chamberlin, M. J. (1988) Structure and function of bacterial sigma factors, *Annu. Rev. Biochem. 57*, 839−872.
16. Hong, Z., Cameron, C. E., Walker, M. P., Castro, C., Yao, N., Lau, J. Y., and Zhong, W. (2001) A novel mechanism to ensure terminal initiation by hepatitis C virus NS5B polymerase, *Virology 285*, 6−11.
17. Hwang, S. B., Park, K. J., Kim, Y. S., Sung, Y. C., and Lai, M. M. (1997) Hepatitis C virus NS5B protein is a membrane-associated phosphoprotein with a predominantly perinuclear localization, *Virology 227*, 439−446.
18. Ivashkina, N., Wolk, B., Lohmann, V., Bartenschlager, R., Blum, H. E., Penin, F., and Moradpour, D. (2002) The hepatitis C virus RNA-dependent RNA polymerase membrane insertion sequence is a transmembrane segment, *J. Virol. 76*, 13088−13093.
19. Johnson, T. L., and Chamberlin, M. J. (1994) Complexes of yeast RNA polymerase II and RNA are substrates for TFIIS-induced RNA cleavage, *Cell 77*, 217−224.
20. Kao, C. C., Yang, X., Kline, A., Wang, Q. M., Barket, D., and Heinz, B. A. (2000) Template requirements for RNA synthesis by a recombinant hepatitis C virus RNA-dependent RNA polymerase, *J. Virol. 74*, 11121−11128.
21. Kolykhalov, A. A., Mihalik, K., Feinstone, S. M., and Rice, C. M. (2000) Hepatitis C virus-encoded enzymatic activities and conserved RNA elements in the 3′ nontranslated region are essential for virus replication in vivo, *J. Virol. 74*, 2046−2051.
22. Koonin, E. V. (1993) A common set of conserved motifs in a vast variety of putative nucleic acid-dependent ATPases including MCM proteins involved in the initiation of eukaryotic DNA replication, *Nucleic Acids Res. 21*, 2541−2547.
23. Kumar, A., Casas-Finet, J. R., Luneau, C. J., Karpel, R. L., Merrill, B. M., Williams, K. R., and Wilson, S. H. (1990) Mammalian heterogeneous nuclear ribonucleoprotein A1. Nucleic acid binding properties of the COOH-terminal domain, *J. Biol. Chem. 265*, 17094−17100.
24. Kunkel, T. A., and Bebenek, K. (2000) DNA replication fidelity, *Annu. Rev. Biochem. 69*, 497−529.
25. Lauger, P. (1987) Dynamics of ion transport systems in membranes, *Physiol. Rev. 67*, 1296−1331.
26. Lee, K. J., Ou, C. J., and Lai, M. C. (2003) The C-terminal transmembrane domain of hepatitis C virus RNA polymerase is essential for HCV replication in vivo, *J. Virol. 78*, 3797−3802.
27. Lesburg, C. A., Cable, M. B., Ferrari, E., Hong, Z., Mannarino, A. F., and Weber, P. C. (1999) Crystal structure of the RNA-dependent RNA polymerase from hepatitis C virus reveals a fully encircled active site, *Nat. Struct. Biol. 6*, 937−943.
28. Leveque, V. J., Johnson, R. B., Parsons, S., Ren, J., Xie, C., Zhang, F., and Wang, Q. M. (2003) Identification of a C-terminal regulatory motif in hepatitis C virus RNA-dependent RNA polymerase: Structural and biochemical analysis, *J. Virol. 77*, 9020−9028.
29. Lohmann, V., Korner, F., Herian, U., and Bartenschlager, R. (1997) Biochemical properties of hepatitis C virus NS5B RNA-dependent RNA polymerase and identification of amino acid sequence motifs essential for enzymatic activity, *J. Virol. 71*, 8416−8428.

30. Lohmann, V., Korner, F., Koch, J., Herian, U., Theilmann, L., and Bartenschlager, R. (1999) Replication of subgenomic hepatitis C virus RNAs in a hepatoma cell line, *Science 285*, 110−113.
31. Lohmann, V., Overton, H., and Bartenschlager, R. (1999) Selective stimulation of hepatitis C virus and pestivirus NS5B RNA polymerase activity by GTP, *J. Biol. Chem. 274*, 10807−10815.
32. Merrill, B. M., Stone, K. L., Cobianchi, F., Wilson, S. H., and Williams, K. R. (1988) Phenylalanines that are conserved among several RNA-binding proteins form part of a nucleic acid-binding pocket in the A1 heterogeneous nuclear ribonucleoprotein, *J. Biol. Chem. 263*, 3307−3313.
33. Milligan, J. F., Groebe, D. R., Witherell, G. W., and Uhlenbeck, O. C. (1987) Oligoribonucleotide synthesis using T7 RNA polymerase and synthetic DNA templates, *Nucleic Acids Res. 15*, 8783−8798.
34. Oh, J. W., Ito, T., and Lai, M. M. (1999) A recombinant hepatitis C virus RNA-dependent RNA polymerase capable of copying the full-length viral RNA, *J. Virol. 73*, 7694−7702.
35. Oh, J. W., Sheu, G. T., and Lai, M. M. (2000) Template requirement and initiation site selection by hepatitis C virus polymerase on a minimal viral RNA template, *J. Biol. Chem. 275*, 17710−17717.
36. O'Reilly, E. K., and Kao, C. C. (1998) Analysis of RNA-dependent RNA polymerase structure and function as guided by known polymerase structures and computer predictions of secondary structure, *Virology 252*, 287−303.
37. Rajendran, K. S., and Nagy, P. D. (2003) Characterization of the RNA-binding domains in the replicase proteins of tomato bushy stunt virus, *J. Virol. 77*, 9244−9258.
38. Ranjith-Kumar, C. T., Gajewski, J., Gutshall, L., Maley, D., Sarisky, R. T., and Kao, C. C. (2001) Terminal nucleotidyl transferase activity of recombinant *Flaviviridae* RNA-dependent RNA polymerases, implication for viral RNA synthesis, *J. Virol. 75*, 8615−8623.
39. Ranjith-Kumar, C. T., Gutshall, L., Sarisky, R. T., and Kao, C. C. (2003) Multiple interactions within the hepatitis C virus RNA polymerase repress primer-dependent RNA synthesis, *J. Mol. Biol. 330*, 675−685.
40. Rhodes, G., and Chamberlin, M. J. (1974) Ribonucleic acid chain elongation by *Escherichia coli* ribonucleic acid polymerase. I. Isolation of ternary complexes and the kinetics of elongation, *J. Biol. Chem. 249*, 6675−6683.
41. Schmidt-Mende, J., Bieck, E., Hugle, T., Penin, F., Rice, C. M., Blum, H. E., and Moradpour, D. (2001) Determinants for membrane association of the hepatitis C virus RNA-dependent RNA polymerase, *J. Biol. Chem. 276*, 44052−44063.
42. Shi, S. T., Lee, K. J., Aizaki, H., Hwang, S. B., and Lai, M. M. (2003) Hepatitis C virus RNA replication occurs on a detergent-resistant membrane that cofractionates with caveolin-2, *J. Virol. 77*, 4160−4168.
43. Siegel, R. W., Adkins, S., and Kao, C. C. (1997) Sequence-specific recognition of a subgenomic RNA promoter by a viral RNA polymerase, *Proc. Natl. Acad. Sci. U.S.A. 94*, 11238−11243.
44. Steiner, T., Kaiser, J. T., Marinkovic, S., Huber, R., and Wahl, M. C. (2002) Crystal structures of transcription factor NusG in light of its nucleic acid- and protein-binding activities, *EMBO J. 21*, 4641−4653.
45. Vo, N. V., Oh, J. W., and Lai, M. M. (2003) Identification of RNA ligands that bind hepatitis C virus polymerase selectively and inhibit its RNA synthesis from the natural viral RNA templates, *Virology 307*, 301−316.
46. Vo, N. V., Young, K. C., and Lai, M. M. (2003) Mutagenic and inhibitory effects of ribavirin on hepatitis C virus RNA polymerase, *Biochemistry 42*, 10462−10471.
47. Wang, Q. M., Hockman, M. A., Staschke, K., Johnson, R. B., Case, K. A., Lu, J., Parsons, S., Zhang, F., Rathnachalam, R., Kirkegaard, K., and Colacino, J. M. (2002) Oligomerization and cooperative RNA synthesis activity of hepatitis C virus RNA-dependent RNA polymerase, *J. Virol. 76*, 3865−3872.
48. Zhong, W., Ferrari, E., Lesburg, C. A., Maag, D., Ghosh, S. K., Cameron, C. E., Lau, J. Y., and Hong, Z. (2000) Template/primer requirements and single nucleotide incorporation by hepatitis C virus nonstructural protein 5B polymerase, *J. Virol. 74*, 9134−9143.

BI049773G